

Supporting Information

Deep Eutectic Solvents Infused Two-Dimensional Metal-Organic Frameworks Membranes as Quasi-Solid-State Electrolytes for Wearable Micro-Supercapacitors

Xiaoyu Wang,^{a, b} Yuqi Wang,^{*a, b} Yuan Kang,^c Bing Yao,^{a, b} Xinsheng Peng^{*a, b}

^a State Key Laboratory of Silicon Materials and Advanced Semiconductor Materials, School of Materials Science and Engineering, Zhejiang University, Hangzhou 310027, China.

^b Wenzhou Key Laboratory of Novel Optoelectronic and Nanomaterials, Institute of Wenzhou, Zhejiang University, Wenzhou 325006, China.

^c Department of Chemical Engineering, Monash University, Clayton, Victoria 3800, Australia

*Corresponding author. E-mail: yuqi.wang@zju.edu.cn; pengxinsheng@zju.edu.cn.

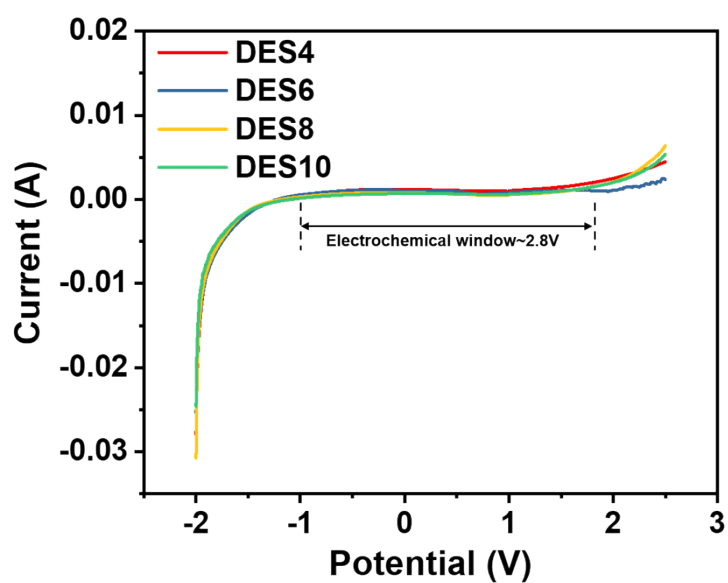


Figure S1. Linear Sweep Voltammetry curve of DES electrolytes at a scanning rate of 10 mV/s.

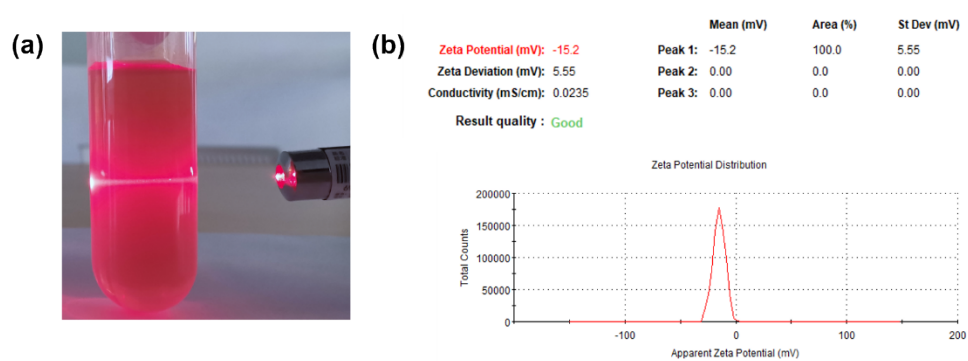


Figure S2. (a) Tyndall effect image of the colloidal suspension of CuTCPP nanosheets.

(b) Zeta potential of CuTCPP nanosheets.

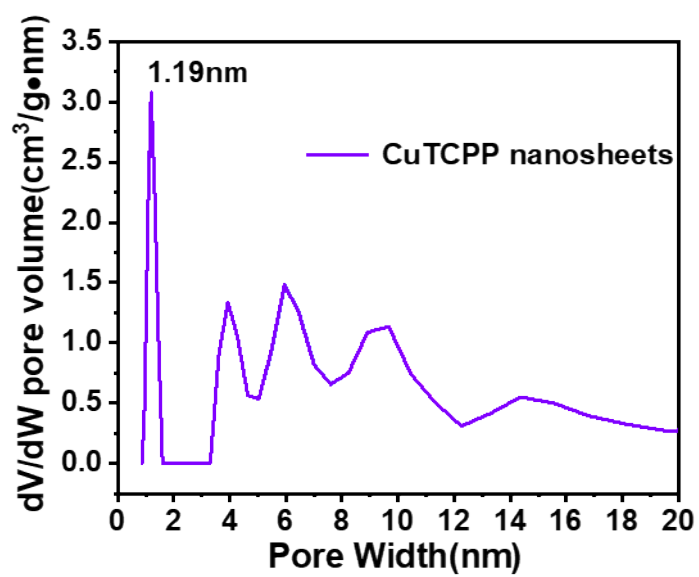


Figure S3. Pore size distribution of CuTCPP nanosheets.

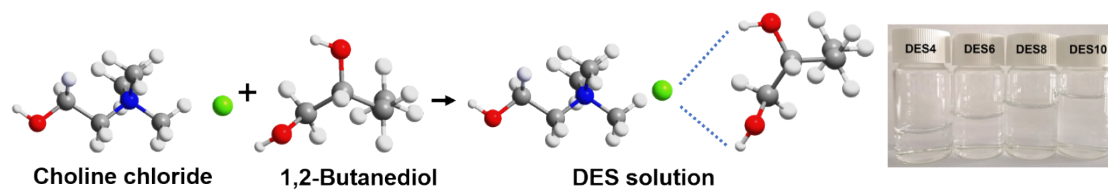


Figure S4. The molecular representation and synthesis of the choline chloride-1,2-butanediol DES, the digital photo of the DES solutions.

Table S1. Molecule sizes of DES and its components after dissociation.

Compounds	Molecule size (Å)	Reference
Choline Chloride	2.3680	1
1,2-butanediol	2.8260	2
Chloride ion	1.8200	3
Choline ion	1.9600	3

Generally, ChCl-BD DES is formed by the combination of two constituents generating a new liquid phase containing the Cl⁻-BD hydrogen bond network.⁴

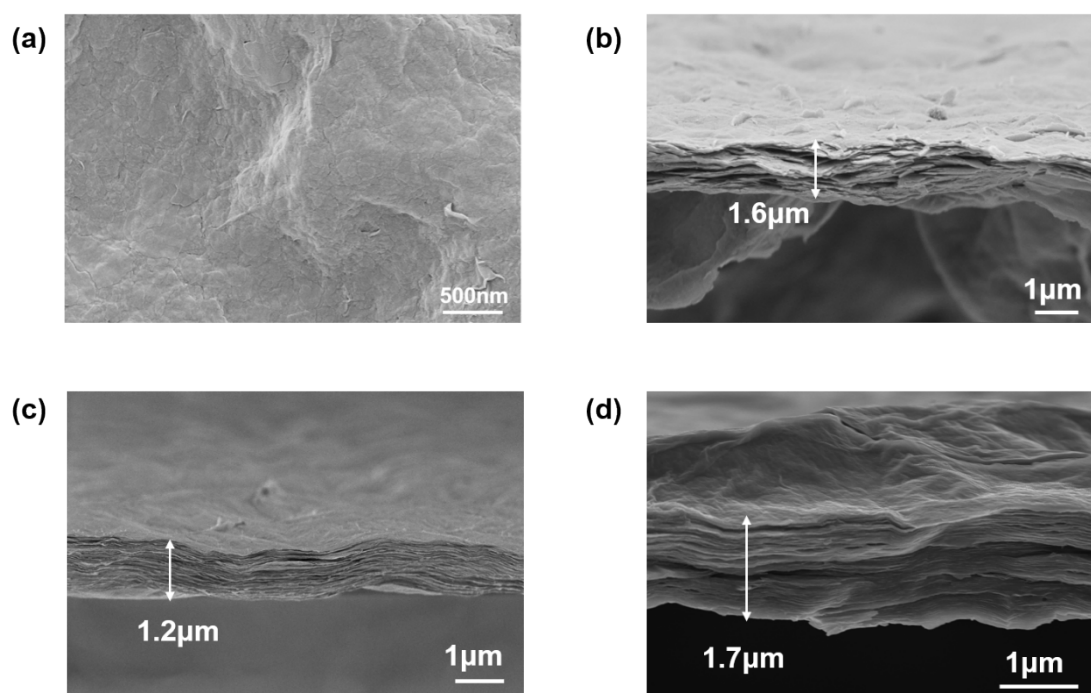


Figure S5. (a) Scanning electronic microscopic (SEM) images of surfaces of CuTCCP membranes. (b) SEM images of cross section of CuTCCP. (c) SEM images of cross section of GO. (d) SEM images of cross section of GO-DES6.

GO nanosheets were fabricated by the common modified Hummers' method.⁵ After DES enter the nanochannel of GO nanosheets, the membrane thickness has increased from 1.2 μm to 1.7 μm .

Table S2. Contents of C 1s, O 1s, N 1s and Cu 2p of CuTCCP membrane.

	Binding Energy (eV)	Atomic (%)
C 1s	284.80	76.42
O 1s	532.04	13.88
N 1s	398.79	6.87
Cu 2p	935.30	26.51

Table S3. Contents of C 1s, O 1s, N 1s, Cu 2p and Cl 2p of CuTCPP-DES6 membrane.

	Binding Energy (eV)	Atomic (%)
C 1s	284.80	74.84
O 1s	532.04	14.33
N 1s	398.78	7.16
Cu 2p	935.15	2.08
Cl 2p	197.62	1.6

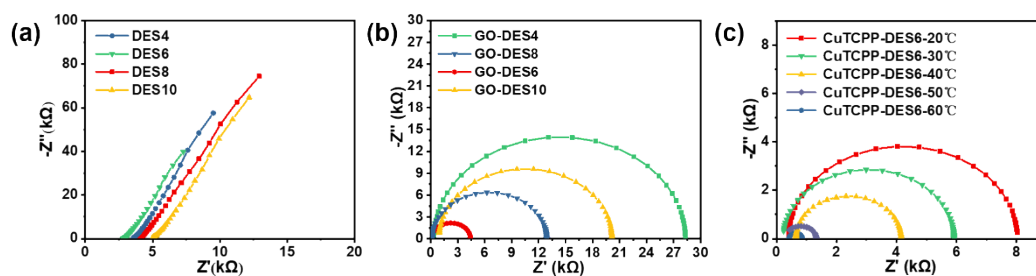


Figure S6. (a) Nyquist plots of DES at room temperature. (b) Nyquist plots of GO-DES membrane at room temperature. (c) Nyquist plots of CuTCPP-DES6 membrane at different temperatures.

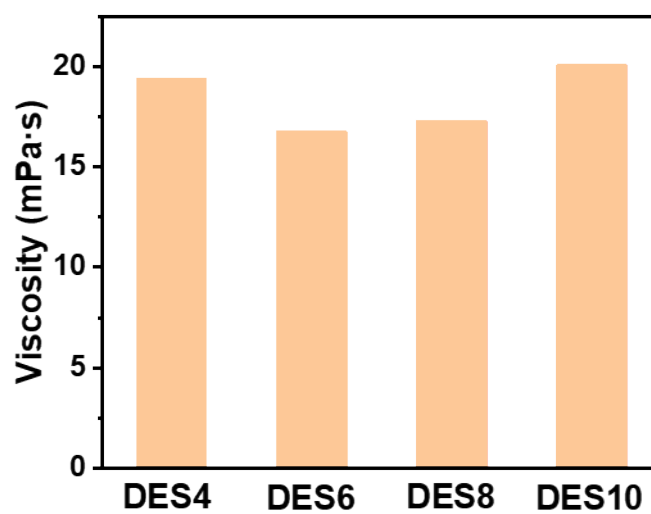


Figure S7. Viscosity pattern of bulk DES system.

The viscosity of DES was measured with a capillary viscometer at room temperature. Three capillaries of an internal diameter of 1.0, 1.5 and 2.5 mm were employed to perform the measurements for the range of viscosity of interest. The viscometer was calibrated with the standards provided by the manufacturer.

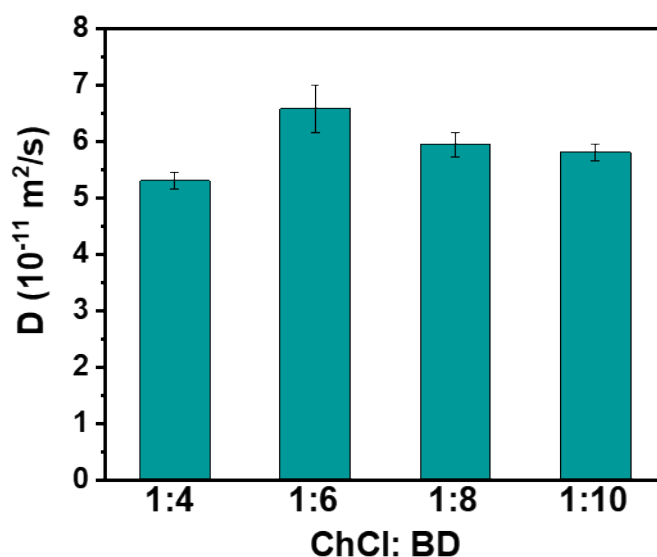


Figure S8. Self-diffusion coefficients of different molar ratio DESs under CuTCCP nanoconfinement

The diffusion coefficients measured by pulsed-field gradient nuclear magnetic resonance (PFG-NMR) were obtained by recording NMR signals at varying magnetic field gradient strengths. The PFG-NMR measurements were obtained on a 700 MHz nuclear magnetic resonance spectrometer (AVANCE NEO, Bruker company). The sweeping range of ^1H is 0–7 ppm.

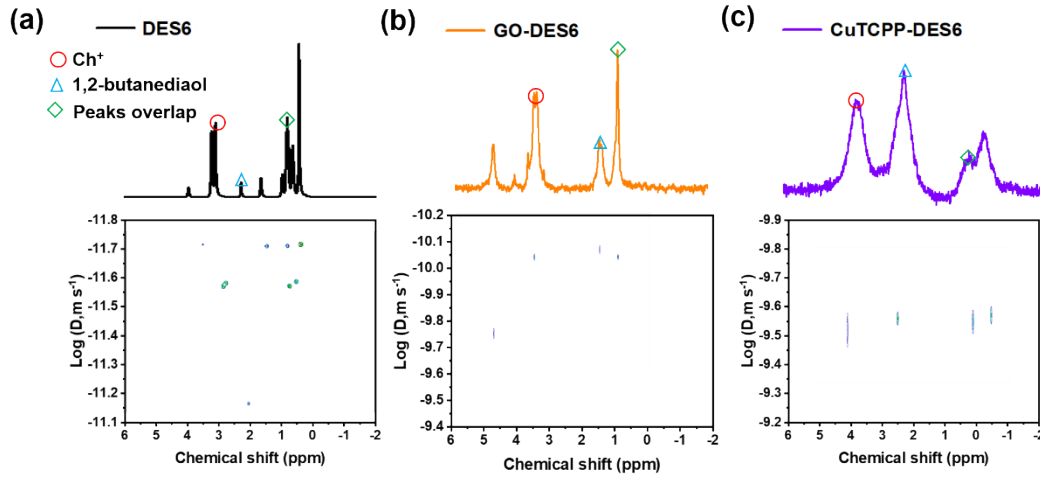


Figure S9. (a-c) ^1H nuclear magnetic resonance (NMR) diffusion ordered spectroscopy (DOSY) spectra of DES6, GO-DES6 and CuTCPP-DES6 membrane at 298 K.

The diffusion coefficients measured by pulsed-field gradient nuclear magnetic resonance (PFG-NMR) were obtained by recording NMR signals at varying magnetic field gradient strengths. Then, the diffusion coefficient can be obtained by plotting the attenuated signal with the Stejskal-Tanner equation below.^{6,7}

$$I = I_0 \exp \left[- (\gamma g \delta)^2 \Delta' D \right] \quad (1)$$

where I and I_0 are final and initial signals, γ is the gyromagnetic ratio of the probed nucleus, g is the magnetic field gradient strengths, δ is the gradient pulse duration, and Δ' is a corrected diffusion time depending on the pulse sequence and the gradient shape. All the other parameters are either fixed in the pulse sequence (γ , δ , Δ') or measured (I , I_0) with the exception of the diffusion coefficient D .

Table S4. Chemical shift and error of diffusion coefficients for peaks of DES6 recorded from ¹H DOSY NMR at 298 K.

Peak name	Chemical Shift(ppm)	Diffusion Coefficient (10 ⁻¹¹ m ² s ⁻¹)	Error (10 ⁻¹⁵)
1	4.279	2.31	4.342
2	3.837	1.19	8.796
3	3.762	0.26	7.141
4	3.267	2.64	1.837
5	2.884	2.28	1.712
6	2.471	1.58	1.545
7	0.343	1.86	6.344

Table S5. Chemical shift and error of diffusion coefficients for peaks of GO-DES6 recorded from ¹H DOSY NMR at 298 K.

Peak name	Chemical Shift(ppm)	Diffusion Coefficient (10 ⁻¹¹ m ² s ⁻¹)	Error (10 ⁻¹²)
1	3.504	6.01	6.708
2	0.863	5.99	6.100
3	1.430	4.98	1.043
4	4.792	4.87	5.724

Table S6. Chemical shift and error of diffusion coefficients for peaks of CuTCPP-DES6 recorded from ^1H DOSY NMR at 298 K.

Peak name	Chemical Shift(ppm)	Diffusion Coefficient ($10^{-11} \text{ m}^2 \text{ s}^{-1}$)	Error (10^{-13})
1	3.731	7.15	4.810
2	2.393	6.37	3.060
3	0.382	6.61	6.925
4	-0.113	6.20	4.392

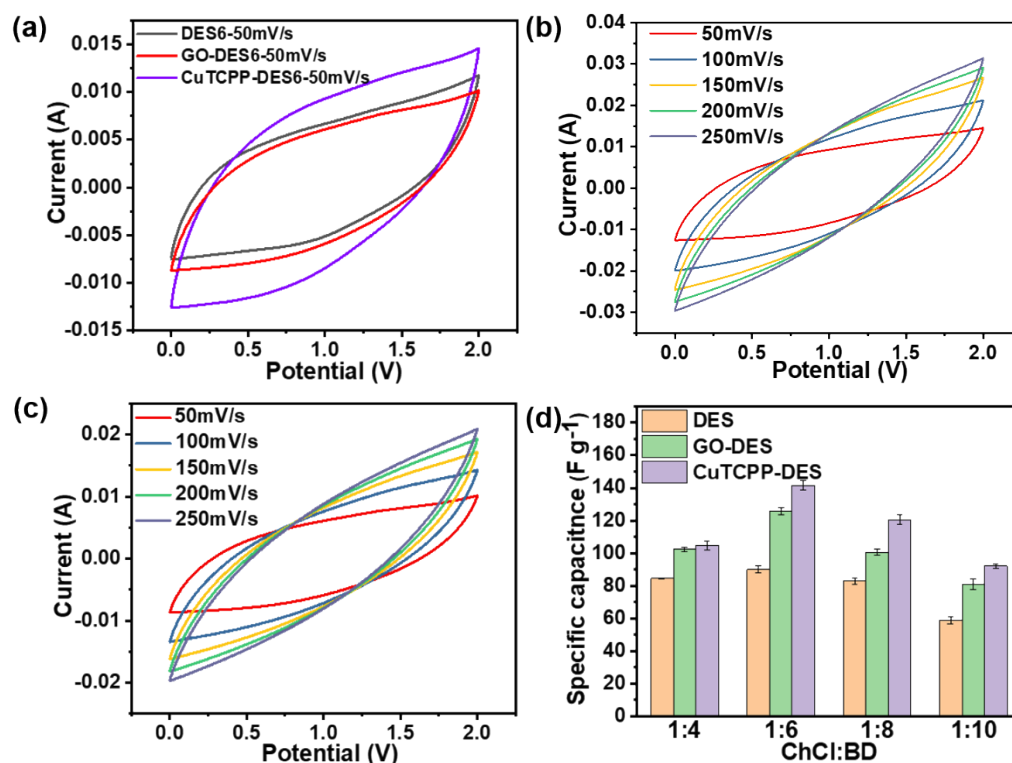


Figure S10. (a) CV at 50 mV/s of DES6, GO-DES6, CuTCPP-DES6 coin cell supercapacitor. (b) CV at different scanning rates from 50 mV/s to 250 mV/s of CuTCPP-DES6 coin cell supercapacitors. (c) CV at different scanning rates from 50 mV/s to 250 mV/s of GO-DES6 coin cell supercapacitors. (d) Capacitance pattern of DES, GO-DES, CuTCPP-DES coin supercapacitor.

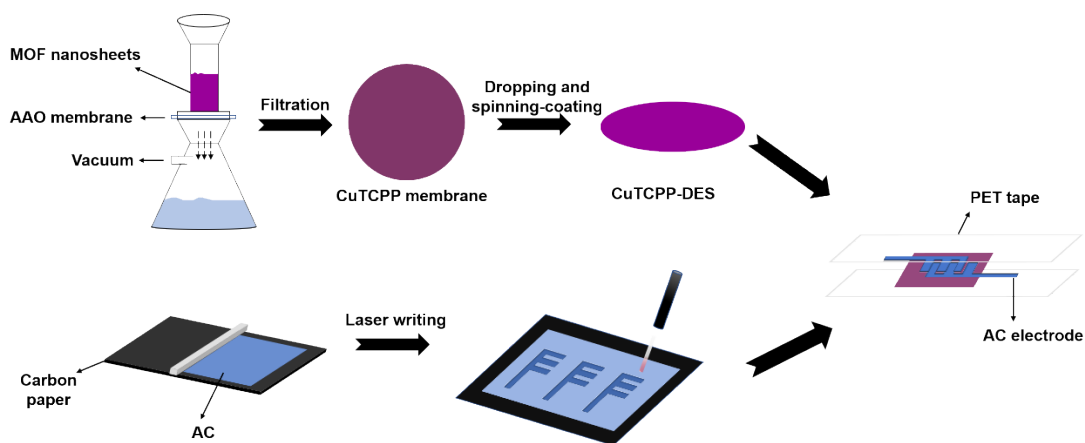


Figure S11. Fabrication process of CuTCPP-DES MSC

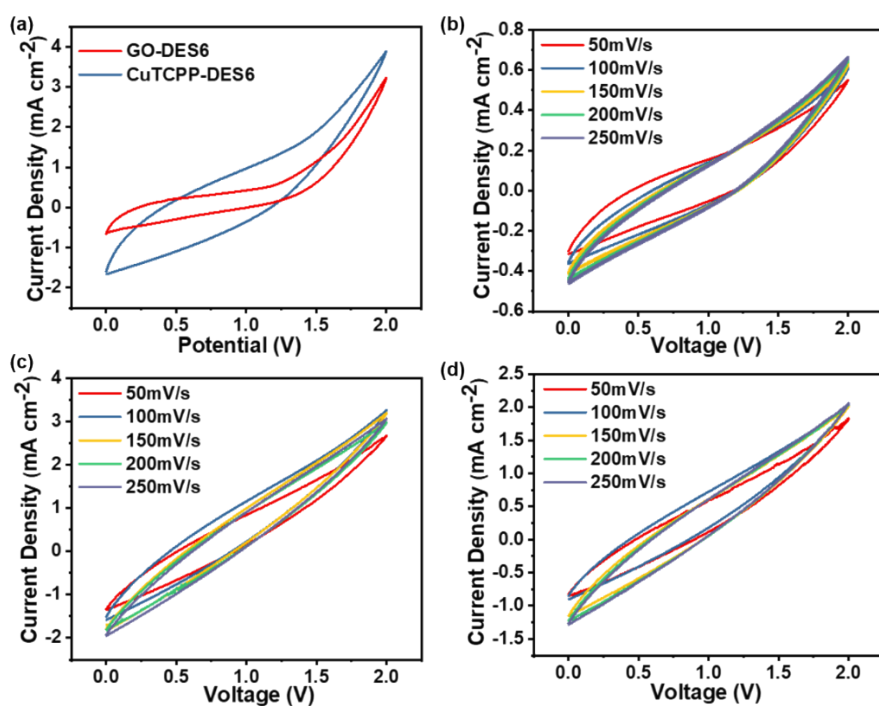


Figure S12. (a) CV at 50 mV/s of GO-DES6 and CuTCPP-DES6 MSCs. (b) CV at different scanning rates of CuTCPP-DES MSC4. (c) CV at different scanning rates of CuTCPP-DES MSC8. (d) CV at different scanning rates of CuTCPP-DES MSC10.

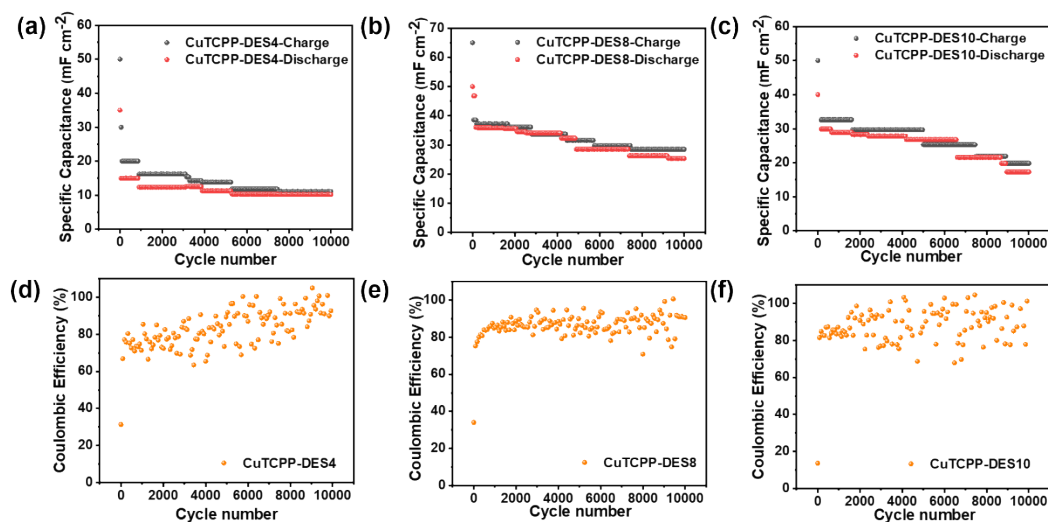


Figure S13. (a-c) Cyclic Charge-Discharge tests of capacitance retention of CuTCPP-DES4 MSC, CuTCPP-DES8 MSC and CuTCPP-DES10 MSC at current density of 1A g⁻¹. (d-f) Coulombic Efficiency of CuTCPP-DES4 MSC, CuTCPP-DES8 MSC and CuTCPP-DES10 MSC during Cyclic Charge-Discharge tests at current density of 1A g⁻¹.

References

- 1 Vincenzo P. Cotroneo-Figueroa, Nicolás F. Gajardo-Parra, Pablo López-Porfiri, Ángel Leiva, Maria Gonzalez-Miquel, José Matías Garrido and Roberto I. Canales, *J. Molecular Liquids*, 2022, **345**, 116986.
- 2 L. F. Zubeir, C. Held, G. Sadowski and M. C. Kroon, *J. Phys. Chem. B*, 2016, **120**, 2300–2310.
- 3 S. Shaukat, M. V. Fedotova, S. E. Kruchinin, M. Bešter-Rogač, Č. Podlipnik and R. Buchner, *Phys. Chem. Chem. Phys.*, 2019, **21**, 10970–10980.
- 4 C. Florindo, F. S. Oliveira, L. P. N. Rebelo, A. M. Fernandes and I. M. Marrucho, *ACS Sus. Chem. Eng.*, 2014, **2**, 2416–2425.
- 5 X. Wang, Y. Wang, M. Dong, Z. Fang, Y. Hu, K. Xue, Z. Ye and X. Peng, *Mater. Today Energy*, 2023, **34**, 101285.
- 6 G. Pagès, V. Gilard, R. Martino and M. Malet-Martino, *Analyst*, 2017, **142**, 3771–3796.
- 7 Y. Wang, W. Chen, Q. Zhao, G. Jin, Z. Xue, Y. Wang and T. Mu, *Phys. Chem. Chem. Phys.*, 2020, **22**, 25760–25768.